Digitoxin inhibits ICC cell properties via the NF-κB/ST6GAL1 signaling pathway

YUEPING ZHAN*, RONG WANG*, CHENJUN HUANG, XUEWEN XU, XIAO XIAO, LINLIN WU, JIAO WEI, TIAN LONG and CHUNFANG GAO

Clinical Laboratory Medicine Center, Yueyang Hospital of Integrated Traditional Chinese and Western Medicine, Shanghai University of Traditional Chinese Medicine, Shanghai 200437, P.R. China

Received March 12, 2024; Accepted May 30, 2024

DOI: 10.3892/or.2024.8762

Abstract. Intrahepatic cholangiocarcinoma (ICC) is a type of liver cancer associated with poor prognosis and increased mortality; the limited treatment strategy highlights the urgent need for investigation. Traditional Chinese Medicine (TCM), used alone or in combination with other treatments, can enhance therapeutic efficacy, improve life quality of patients and extend overall survival. In total, two rounds of screening of a TCM library of 2,538 active compounds were conducted using a Cell Counting Kit-8 assay and ICC cell lines. Cell proliferation and migration abilities were assessed through colony formation, 5-ethynyl-2'-deoxyuridine, would healing and Transwell assays. The impact of digitoxin (DT) on signaling pathways was initially investigated using RNA sequencing and further validated using reverse transcription-quantitative PCR, western blotting, lectin blotting and flow cytometry. ICC cells stably overexpressing ST6 β-galactoside α-2,6-sialyltransferase 1 (ST6GAL1) were generated through lentiviral transfection. It was shown that DT emerged as a highly effective anti-ICC candidate from two rounds high-throughput library screening. DT could inhibit the proliferation and migration of ICC cells by suppressing NF-κB activation and reducing nuclear phosphorylated-NF-κB levels, along with diminishing ST6GAL1 mRNA and protein expression. The aforementioned biological effects and signal pathways of DT could be counteracted by overexpressing ST6GAL1 in ICC cells. In conclusion, DT suppressed ICC cell proliferation and migration by targeting the NF-κB/ST6GAL1 signaling axis. The findings of the present study indicated the promising therapeutic effects of DT in managing ICC, offering new avenues for treatment strategies.

Correspondence to: Professor Chunfang Gao, Clinical Laboratory Medicine Center, Yueyang Hospital of Integrated Traditional Chinese and Western Medicine, Shanghai University of Traditional Chinese Medicine, 110 Ganhe Road, Hongkou, Shanghai 200437, P.R. China
E-mail: gaocf1115@163.com

*Contributed equally

Abbreviations: ICC, intrahepatic cholangiocarcinoma; TCM, Traditional Chinese Medicine; ST6GAL1, ST6 β-galactoside α-2,6-sialyltransferase 1; DT, digitoxin; DMSO, dimethyl sulfoxide; OD, optical density; HiBEpiCs, intrahepatic bile duct epithelial cells; EdU, 5-ethynyl-2'-deoxyuridine; RNA-seq, RNA-sequencing; GO, Gene Ontology; KEGG, Kyoto Encyclopedia of Genes and Genomes; SNA, Sambucus nigra; CCK-8, Cell Counting Kit-8; OS, overall survival; CCA, cholangiocarcinoma

Key words: DT, ICC, ST6GAL1, NF-κB, treatment

Introduction

Biliary tract cancers include intrahepatic cholangiocarcinoma (ICC), perihilar, distal cholangiocarcinoma and gall bladder carcinoma based on their location of origin. Notably, ICC stands out as a type of cancer associated with increased mortality. It ranks as the second most prevalent primary liver cancer, constituting ≤20% of liver cancers and 3% of all gastrointestinal cancers (1,2). The prognosis for patients with ICC undergoing surgery with the intent to cure is poor, with a 5-year overall survival (OS) range of 5-17% (3). Patients with unresectable ICC have a median survival of 11.7 months with palliative chemotherapy, primarily gemcitabine and cisplatin (4). Despite the potential of emerging treatments such as triplet regimens, immunotherapy and targeted therapies for specific genetic alterations (5), the persistent challenges of tumor resistance and low OS rates underscore the limited efficacy of current clinical treatments for ICC. Therefore, the development of more effective anti-ICC drugs is critical and pressing issue in medical oncology research to improve treatment outcomes and patient survival.

Natural products continue to be a vital and promising reservoir for chemotherapeutic agent discovery, exemplified by drugs such as artemisinin, an antimalarial agent (6). Between 1981 and 2014, 49% of the anticancer drugs approved by the FDA originated either directly from natural sources or as derivatives. These include notable drugs such as vinblastine and colchicine, highlighting the significant role of natural resources in cancer drug development (7,8). Digitoxin (DT), a cardiac glycoside naturally sourced from species of the genus *Digitalis* (9), has served as an effective Na^+/K^+-ATPase inhibitor. For >4 decades, it has been used in the clinical

management of congestive heart failure (10). Numerous studies have investigated the anticancer effects of DT, revealing its potent antitumor efficacy in a diverse range of cancer types (11-14). However, the ability and underlying mechanism of DT as an anticancer reagent against ICC, a lethal cancer without satisfactory chemotherapy, remains unknown.

In the present study, a screening of a TCM library of 2,538 unique natural compounds was conducted to discover potential lead compounds exhibiting anti-ICC activity. Among the noteworthy compounds discovered, DT emerged as a significant anti-ICC chemotherapeutic agent. The effects of DT on ICC cell proliferation and metastasis were further evaluated through cell functional assays, and the key signaling pathways involved were explored. ST6 β-galactoside α-2,6-sialyltransferase 1 (ST6GAL1), which facilitates the addition of sialic acid to N-glycosylated proteins, is substantially upregulated in various types of malignancies, playing a crucial role in the progression of cancer. It was revealed that the mRNA and protein ST6GAL1 expression in ICC cells was suppressed by DT. Overexpression of ST6GAL1 could reverse the inhibitory effect of DT on ICC. It was shown that DT inhibited ICC cell proliferation and metastasis by targeting the NF-κB/ST6GAL1 signaling pathway. The findings of the present study indicated the therapeutic potential of DT in the treatment of ICC.

Materials and methods

Cell culture. HCCC-9810, RBE and 293T cell lines were obtained from the Chinese Academy of Sciences, Shanghai Branch Cell Bank. HuCCT1 were purchased from Cyagen, and normal human intrahepatic biliary epithelial cells (HiBEpiCs) were obtained from Qingqi (Shanghai) Biotechnology development Co., Ltd. Cells were cultured in RPMI-1640 medium (cat. no. 11875119; Gibco, Thermo Fisher Scientific, Inc.) supplemented with 10% FBS (cat. no. 10099141C; Gibco; Thermo Fisher Scientific, Inc.) and 1% penicillin/streptomycin (cat. no. 15140122; Gibco; Thermo Fisher Scientific, Inc.) at 37˚C in a humidified incubator (HERA cell VIOS; Themo Fisher Scientific, Inc.) with 5% CO_2. 293T cells were cultured in DMEM (cat. no. 11995065; Gibco; Thermo Fisher Scientific, Inc.) supplemented with 10% FBS and 1% penicillin/streptomycin. Dimethyl sulfoxide (DMSO) was obtained from Sigma-Aldrich; Merck KGaA, and DT (cat. no. HY-B1357) was purchased from MedChemExpress.

Cell viability assay. The cell suspension (100 µl/well) was seeded in 96-well culture plates (cat. no. 3599; Corning, Inc.) at a density range of 1-2x10^5 cells/ml. The cells were treated and incubated with DT at serial concentrations for 24, 48 and 72 h. A total of 10 µl CCK-8 (cat. no. HY-K0301; MedChemExpress) solution was then added to each well of the plate. The plate was incubated for 3 h at 37˚C and absorbance was measured at 450 nm using the Molecular Devices Spectra Max iD3 Microplate Detection System. The cell viability rate was calculated as experimental optical density (OD) value/control OD value.

High-throughput screening of TCM library. A total of 2,538 compounds in the TCM Active Compound Library (cat. no. HY-L065; MedChemExpress) were used for the screening experiment. Compounds were initially screened at a concentration of 10 µM. A further screening was conducted with the criterion that ICC cell viability should be decreased by 70% compared with the control (DMSO). Subsequently, compounds that maintained a viability rate >80% in HiBEpiCs were selected as candidates for anti-ICC drugs.

Overexpression of ST6GAL1 in ICC cells. The overexpression of ST6GAL1 plasmids and control plasmids (pHBLV-CMV-MCS-3FLAG-EF1-ZsGreen-T2A-PURO) was carried out by Hanbio Biotechnology Co., Ltd. For the construction of the ST6GAL1-overexpression cell line, transfer plasmid (10 µg; A260/A280=1.94), envelope plasmid (pMD2G, 5 µg; A260/A280=1.93) and packaging plasmids (pSPAX2, 10 µg; A260/A280=1.92) were co-transfected into 293T packaging cells using Lipofectamine 3000 (cat. np. L3000015; Thermo Fisher Scientific, Inc.) according to the manufacturer's instructions at 37˚C. The culture medium was replenished 16 h later, and the culture supernatant was collected at 2 and 3 days. The virus supernatant was centrifuged in a 50-ml centrifuge tube at 4˚C and 2,000 x g for 10 min to remove cell debris. Then, the clarified viral supernatant was collected and placed into an ultracentrifuge tube to be centrifuged at 4˚C and 82,700 x g for 120 min. The viral pellet was resuspended in 400 µl complete medium and finally the resuspended solution was aliquoted into sterilized viral tubes. A total of 2x10^5 HCCC-9810 or HuCCT1 cells were seeded in 12-well plates overnight and subsequently infected with 50 µl lentivirus expressing the ST6GAL1 gene or a control lentivirus. The transfected cells were screened using puromycin (1 µg/ml) 1 week later.

Overexpression of P65/NF-κB in 293T cells. The overexpression of P65/NF-κB plasmids and control plasmids pcDNA3.1 was carried out by Hanbio Biotechnology Co., Ltd. The P65/NF-κB overexpression plasmids (4 µg; A260/A280=1.93) were transfected into 293T cells at 37˚C using Lipofectamine 3000 (cat. np. L3000015; Thermo Fisher Scientific, Inc.) according to the manufacturer's instructions. The medium was refreshed 6 h after transfection, 50 nM DT was added 24 h post-transfection, and WB and RT-qPCR were performed at 48 h.

Colony formation and 5-ethynyl-2'-deoxyuridine (EdU) assays. A total of 1,000 ICC cells/well treated with different concentrations of DT and the ST6GAL1-overexpressed ICC cells treated with DT were plated in 12-well plates (cat. no. 3513; Corning, Inc.) and cultured at 37˚C for 7 days. Subsequently, they were fixed in 4% paraformaldehyde (w/v) for 10 min at RT. After washing three times with PBS, staining was performed using 0.1% crystal violet staining solution (cat. no. C0121; Beyotime Institute of Biotechnology) for 10 min at room temperature (RT). Images were captured using a BZ-X800 fluorescence microscope (Keyence Corporation), and the colonies with aggregates of ≥50 cells were counted.

The ICC cells treated with different concentrations of DT and the ST6GAL1-overexpressed ICC cells treated with DT were seeded into a 24-well plate (cat. no. 3524; Corning, Inc.). Cell proliferation was assessed by incorporating EdU (cat. no. C0071S; Beyotime Institute of Biotechnology) following the manufacturer's instructions. The percentage of

EdU^+ cells was calculated by three random images captured with the BZ-X800 microscope.

Wound healing assay. The ICC cells treated with different concentrations of DT and the ST6GAL1-overexpressing ICC cells treated with DT were seeded in 12-well plates and allowed to incubate for 1 day. When the cells reached ~90% confluence, the bottom of each well was scratched with a 10-μl pipette tip. After washing with PBS, the culture medium was replenished with serum-free medium for culture. Images were captured under an inverted light microscope (cat. no. DMi8; Leica Microsystems) at 0 and 24 h, and the migration area was computed using ImageJ software (version 1.53a; National Institutes of Health).

Cell migration. The ICC cells treated with different concentrations of DT and the ST6GAL1-overexpressing ICC cells treated with DT were collected and diluted with serum-free DMEM to a concentration of $1x10^5$ cells/ml. The upper chamber (8 μm; cat. no. 353097; Falcon; Corning, Inc.) was filled with 200 μl cell suspension in order to measure the capacity for migration. The migratory cells were subsequently stained with 0.1% crystal violet staining solution for 10 min at RT and observed using a BZ-X800 microscope. The number of migratory cells was counted using three randomly selected images of selected fields.

RNA sequencing (RNA-seq). RNA-seq and analysis were conducted by Shanghai Biotechnology Co., Ltd. RNA extraction was performed using the MJzol Animal RNA Isolation Kit (Majorivd; https://www.majorbio.com/shop/goods/71), followed by purification with the RNAClean XP Kit (Beckman Coulter, Inc.) and RNase-Free DNase Set (Qiagen, Inc.). RNA integrity and quality (260/280 nm ratio >1.8) were assessed using the Agilent 2100 Bioanalyzer/Agilent 4200 TapeStation and quantified with the Qubit 2.0® Fluorometer (Thermo Fisher Scientific, Inc.) and NanoDrop ND-2000 (Thermo Fisher Scientific, Inc.). The mRNA was isolated from the purified RNA, fragmented and synthesized into cDNA, with subsequent library construction steps including end repair, adenylation, adapter ligation and enrichment. Purified libraries were quantified by Qubit® 2 .0 Fluorometer (Thermo Fisher Scientific, Inc.) and validated by Agilent 2100 bioanalyzer (Agilent Technologies, Inc.) to confirm the insert size and calculate the mole concentration. Cluster was generated by cBot with the library diluted to 10 pM and then were sequenced on the Illumina NovaSeq6000 platform (Illumina, Inc.) with the PE150 (Pair-end 150 bp) mode. Following data analysis at the transcript level and differential gene screening, differentially expressed genes were identified. Subsequent analyses were carried out to determine the Gene Ontology (GO) functional significance and Kyoto Encyclopedia of Genes and Genomes (KEGG) pathway significance.

Reverse transcription-quantitative PCR (RT-qPCR). The EZ-press RNA purification kit (cat. no. B0004D; EZBioscience) was used to extracted total RNA from cells. The concentration of the extracted RNA was measured by NanoDrop (Thermo Fisher Scientific, Inc.) at 260 nm. PrimeScript™ RT Reagent Kit (cat. no. RR037A; Takara Bio, Inc.) was applied to reverse transcribe RNA into cDNA according to the manufacturer's protocol. Each RT reaction contained 500 ng RNA. TB Green™ Premix Ex Taq™ (cat. no. RR420A; Takara Bio, Inc.) was used for qPCR, and data collection and analysis were carried out using an Applied Biosystems PCR System (7500 Real-Time PCR System; Thermo Fisher Scientific, Inc.). The PCR thermocycling conditions were as follows: i) Stage 1, 95˚C for 30 sec; ii) Stage 2, 95˚C for 5 sec, 60˚C for 34 sec, 40 cycles; iii) Stage 3, 95˚C for 30 sec, 60˚C for 1 min, 95˚C for 15 sec. The $2^{-\Delta\Delta Cq}$ method (15) was used to ascertain the relative expression levels of each gene, with GAPDH serving as the internal reference. Primer sequences were as follows: ST6GAL1 forward, 5'-CCCCAATCAGCCCTTTTACATCCTC-3' and reverse, 5'-CCTGGTCACACAGCGTCATCATG-3'; and GAPDH forward, 5'-CCAGCAAGAGCACAAGAGGAAGAG-3' and reverse, 5'-GGTCTACATGGCAACTGTGAGGAG-3'.

Western blotting and lectin blotting. Cells treated with different concentrations of DT were lysed using cell lysis buffer (cat. no. 9803s; Cell Signaling Technology, Inc.) containing ProtLytic Protease and Phosphatase Inhibitor Cocktail (cat. no. P002; NCM Biotech). Nuclear proteins were extracted using the Nuclear and Cytoplasmic Protein Extraction Kit (cat. no. P0028; Beyotime Institute of Biotechnology). The protein concentrations were quantified by the BCA protein assay kit (cat. no. P0011; Beyotime Institute of Biotechnology). A total of 30 μg proteins were separated by 7.5 or 10% SDS-PAGE, and the resulting proteins were then moved from the gel onto PVDF membranes (cat. no. ISEQ00010; MilliporeSigma).

After 1 h of incubation with 5% skimmed milk at RT, membranes were incubated with primary antibodies against Bcl-2 (1:1,000; cat. no. 12789-1-AP; Proteintech Group, Inc.), ST6GAL1 (1 μg/ml; cat. no. AF5924; R&D Systems, Inc.), BAX (1:1,000; cat. no. 50599-2-Ig; Proteintech Group, Inc.), phosphorylated (p)-NF-κB p65 (1:1,000; cat. no. 3033; Cell Signaling Technology, Inc.), NF-κB p65 (1:1,000; cat. no. 8242; Cell Signaling Technology, Inc.), p-p38 MAPK (1:1,000; cat. no. 4511; Cell Signaling Technology, Inc.), p38 MAPK (1:1,000; cat. no. 8690; Cell Signaling Technology, Inc.), GAPDH (1:5,000; cat. no. 10494-1-AP; Proteintech Group, Inc.) and biotinylated *Sambucus nigra* (SNA) lectin recognizing α2,6-linked sialic acid (1:2,000; cat. no. B-1305; Vector Laboratories) at 4˚C overnight. The membranes were then incubated with secondary antibodies at RT, goat anti-rabbit (1:5,000; cat. no. 7074; Cell Signaling Technology, Inc.), goat anti-mouse (1:5,000; cat. no. 7076; Cell Signaling Technology, Inc.), or streptavidin-HRP (1:5,000; cat. no. 3999; Cell Signaling Technology, Inc.). Protein visualization was carried out using a chemiluminescence ECL Detection kit (NcmECL Ultra; cat. no. P10300; NCM). The software used for densitometric analysis was ImageJ software (version 1.53a; National Institutes of Health).

In situ fluorescence detection of α2,6-linked sialic acid. The ICC cells treated with varying concentrations of DT and the DT-treated ST6GAL1-overexpressing ICC cells were fixed for 10 min with 4% paraformaldehyde at RT. Following fixation, cells were blocked for 1 h using blocking buffer (cat. no. P0260;

Beyotime Institute of Biotechnology) for immunological staining at RT. Next, the cells were incubated with Cy5 labeled SNA lectin (cat. no. CL-1305-1; Vector Laboratories) overnight at 4˚C. Each step involved washing three times with PBS for 5 min. Finally, the slides were sealed using an antifade mounting medium containing 1 μg/ml DAPI (cat. no. A4084; UElandy; http://www.uelandy.com/productDe_235.html); then images were captured by a BZ-X800 microscope.

Flow cytometry. After harvesting ICC cells with ST6GAL1 overexpression treated with DT, the cells were blocked for 20 min on ice using a carbo-free blocking solution (cat. no. SP-5040; Vector Laboratories) at a volume of 0.2 ml for $1x10^6$ cells. Subsequently, these cells were incubated with Cy5-labeled SNA lectin (1 μl per $1x10^6$ cells). Cells were analyzed with a BD FACSCanto II Flow Cytometer (BD Biosciences). FlowJo software (version 10.8.1; Becton Dickinson and Company) was used for analysis.

Statistical analysis. GraphPad Prism (version 9; Dotmatics) was used to conduct statistical analyses. Error bars in the experiments represent SD. The legends provide information about the number of events and independent experiments. Statistical comparisons between two experimental conditions were conducted using the Mann-Whitney test or unpaired Student's t-test, and the Wilcoxon rank-sum test was used for all paired samples. A one-way ANOVA was used to compare multiple experimental groups, followed by Tukey's post hoc test. $P<0.05$ was considered to indicate a statistically significant difference.

Results

Screening of monomeric compounds with anti-ICC activity. High-throughput drug screening was performed to evaluate the antitumor properties of TCM monomeric compounds in a TCM Active Compound Library containing 2,538 compounds. The screening aimed to assess the inhibitory effects of these compounds on the viability of ICC. In the initial screening (Fig. S1A), 83 monomers were identified that exhibited a growth inhibition rate >70% in HCCC9810 and RBE cells (Fig. S1B). Through a secondary screening, 64 monomers with consistent inhibitory activity >70% were selected (Fig. S1C). By assessing the viability of HiBEpiCs, 15 active monomers were identified that showed inhibitory effects on ICC without adverse effects on HiBEpiCs (Fig. S1D). DT emerged as a standout among the 15 active compounds tested, showcasing potent anti-ICC cell activity and promising therapeutic potential against ICC.

DT reduces the proliferation of ICC cells. To assess the inhibitory effects of DT on ICC cells, a CCK-8 assay was conducted which allowed to evaluate the impact of varying concentrations and treatment durations of DT on cell viability. The findings revealed a significant dose-dependent reduction in the viability of both HuCCT1 and HCCC9810 cell lines (Fig. 1A). More specifically, the IC_{50} values for HCCC9810 cells after 24, 48 and 72 h of DT treatment were 106.5±23.2, 92.4±12.1 and 77.9±10.9 nM, respectively. For HuCCT1 cells, the corresponding IC_{50} values were 132.3±33.8, 105.1±26.6 and 98.5±4.2 nM, respectively, indicating a progressive decrease in IC_{50} values, which suggests an increase in drug sensitivity over time. Subsequently, to further probe the effects of DT on cell proliferation, a series of concentration gradients were applied: 0, 1/4 IC_{50}, 1/2 IC_{50}, IC_{50} of DT at 48 h (Table SI); and the proliferation capacity of ICC cells was assessed at 24 h. Through the analysis of the colony formation and EdU incorporation assays, it was observed that DT significantly decreased the colony formation and proliferation ability of HuCCT1 and HCCC9810 cells, demonstrating a dose-dependent inhibition (Fig. 1B and C). Taken together, these findings strongly suggest that DT possesses the ability to hinder both the viability and proliferation of ICC cells.

DT suppresses the migration of ICC cells. To explore the potential suppressive impact of DT on the migration capabilities of ICC cells, the cells were exposed to varying concentrations of DT, and wound healing and Transwell assays were carried out. The Transwell assay results showed that DT significantly decreased the migration of HuCCT1 and HCCC9810 cells in a dose-dependent manner ($P<0.05$; Fig. 2A). Additionally, an increase in DT concentration led to a decrease in the migration areas for both HCCC9810 (Fig. 2B) and HuCCT1 (Fig. 2C) cells, underscoring a progressive impediment to cell movement. Collectively, these findings demonstrated the ability of DT to inhibit the migration of ICC cells.

The NF-κB/ST6GAL1 pathway plays a crucial role in the inhibitory effects of DT on ICC cells. Subsequently, the primary signaling pathways through which DT exerted its inhibitory effects on ICC cell functions were investigated. The aim was to delineate the *in vitro* molecular mechanisms underlying the suppression of ICC cell activities with DT. Firstly, the intersection of differentially expressed genes in HCCC9810 and HUCCT1 cells after treatment with DT was selected, including both upregulated and downregulated genes. Subsequently, GO and KEGG functional enrichment analyses were conducted. RNA-seq analysis unveiled significant alterations in pathways related to glycosylation, regulation of NF-κB imported into the nucleus and transcriptional mis-regulation in ICC cells following treatment with DT (Fig. 3A and B). The heatmap of differentially expressed genes suggested that DT could downregulate the transcriptional levels of ST6GAL1 (Fig. 3C). Furthermore, the RT-qPCR results confirmed that DT could effectively inhibit the mRNA expression of ST6GAL1 (Fig. 3D). Next, the effects of DT on the NF-κB, P38 and STAT3 signaling pathways, as well as ST6GAL1 expression were investigated. DT treatment resulted in inhibition of phosphorylation of p-NF-κB and p-STAT3, while it upregulated the phosphorylation of P38 and reduced the expression of the anti-apoptotic protein BCL-2 (Fig. 3E; statistical charts, Fig. S2). It was found that NF-κB interacted with the promoter region of the ST6GAL1 gene, initiating its transcription (16). To confirm the effect of NF-κB on ST6GAL1, a P65/NF-κB overexpression plasmid was constructed, transfected into 293T cells and followed by DT treatment (Fig. S3). The results indicated that overexpression of NF-κB promoted the expression of ST6GAL1, and also demonstrated the inhibitory effect of DT on ST6GAL1

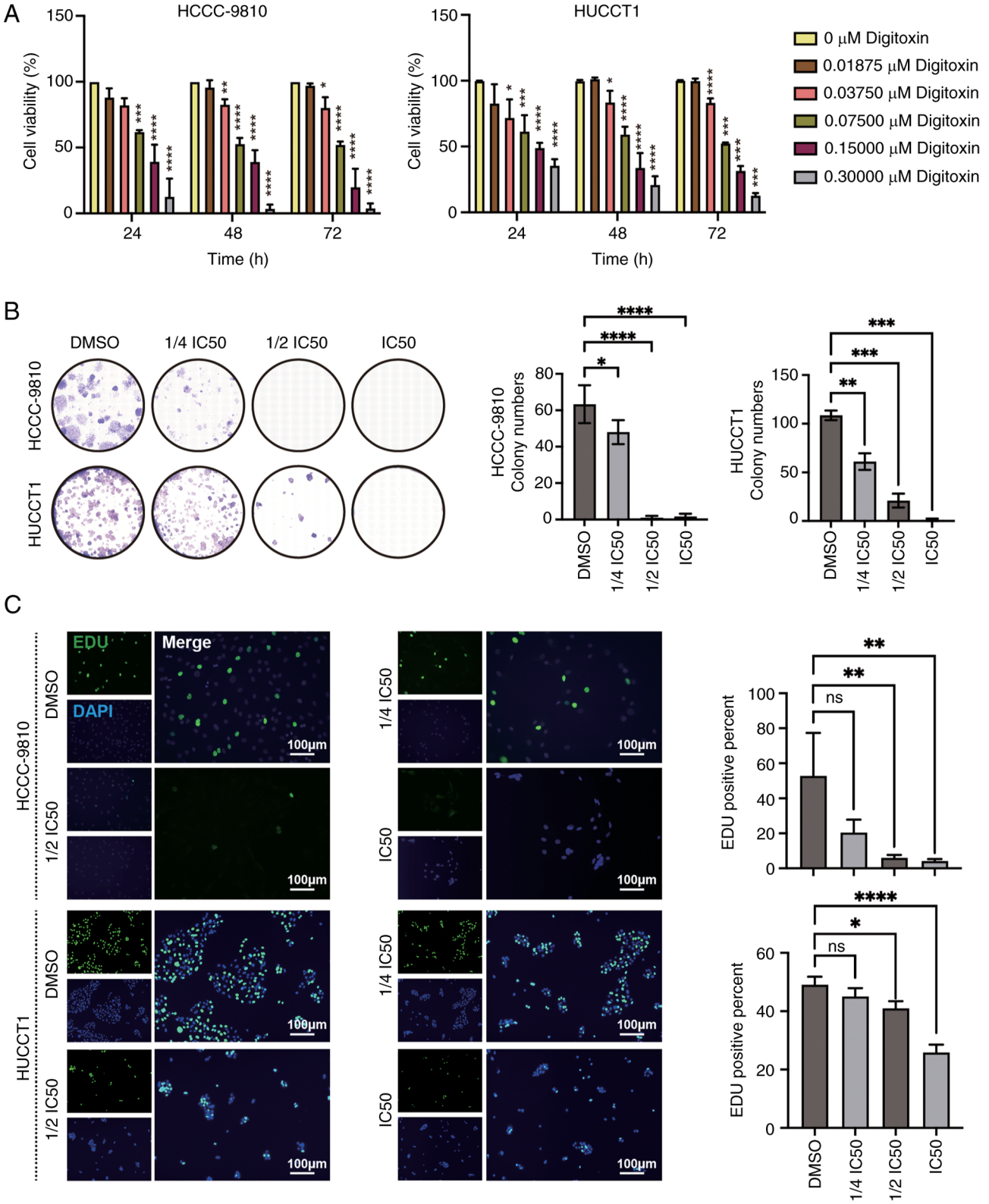

Figure 1. DT effectively suppresses the proliferation of intrahepatic cholangiocarcinoma cells. (A) Cell viability of HCCC9810 and HuCCT1 treated with DT measured using the Cell Counting Kit-8 assay. (B) Colony formation and (C) 5-ethynyl-2'-deoxyuridine assays used to measure cell proliferation. Data are presented as the mean ± SD, representing the results of three independent experiments. *P<0.05, **P<0.01, ***P<0.001 and ****P<0.0001. DT, digitoxin; ns, no significance.

in 293T cells. Finally, lectin blotting with SNA was used which selectively adheres to α2,6-sialic acid structures to evaluate the α2,6-sialylation levels *in situ*. A dose-dependent reduction in α2,6-sialylation, predominantly triggered by DT, was observed (Fig. 3F and G). These findings collectively revealed the involvement of the NF-κB/ST6GAL1 pathway in mediating the effects of DT in ICC cells, underscoring its significance in the modulation of ICC cell abilities.

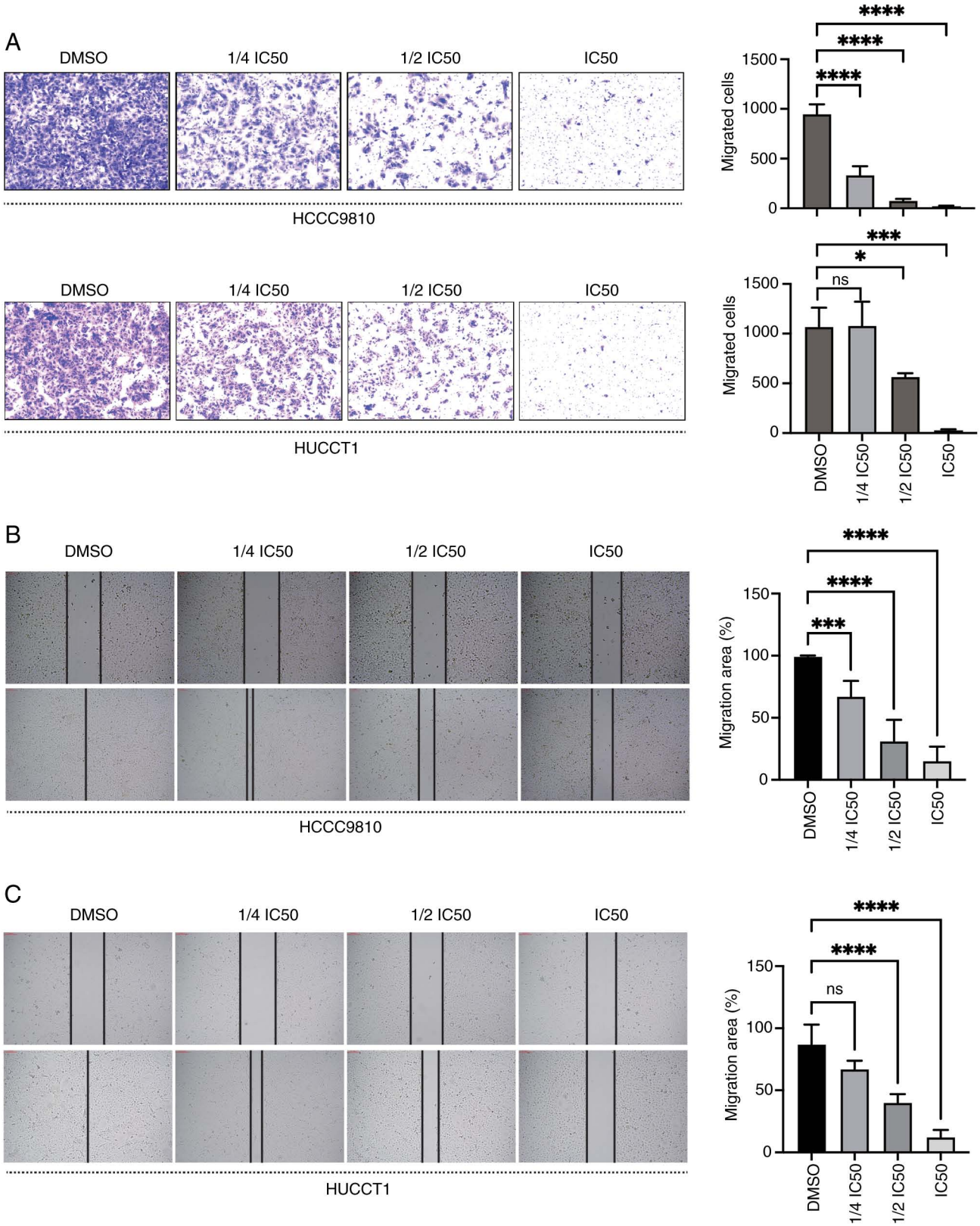

Figure 2. DT suppresses the migration of intrahepatic cholangiocarcinoma cells. (A) Transwell assay detected the migration of HCCC9810 and HuCCT1 treated with DT. (B and C) A wound healing assay was performed to monitor the migration of (B) HCCC9810 and (C) HuCCT1 cells after receiving DT treatment. Error bars represent mean ± SD of three separate experiments. *P<0.05, ***P<0.001 and ****P<0.0001. DT, digitoxin; ns, no significance.

ST6GAL1 counteracts the inhibitory effects of DT on cell proliferation and migration. The aforementioned results revealed that DT reduced the expression of ST6GAL1 in a dose-dependent manner. Consequently, the ability of overexpressing ST6GAL1 to reverse the inhibitory effects of DT on ICC cells was investigated. ST6GAL1-overexpressing-ICC cells were generated by a lentivirus vector system. The increased levels of ST6GAL1 in ST6GAL1-overexpressing HCCC9810

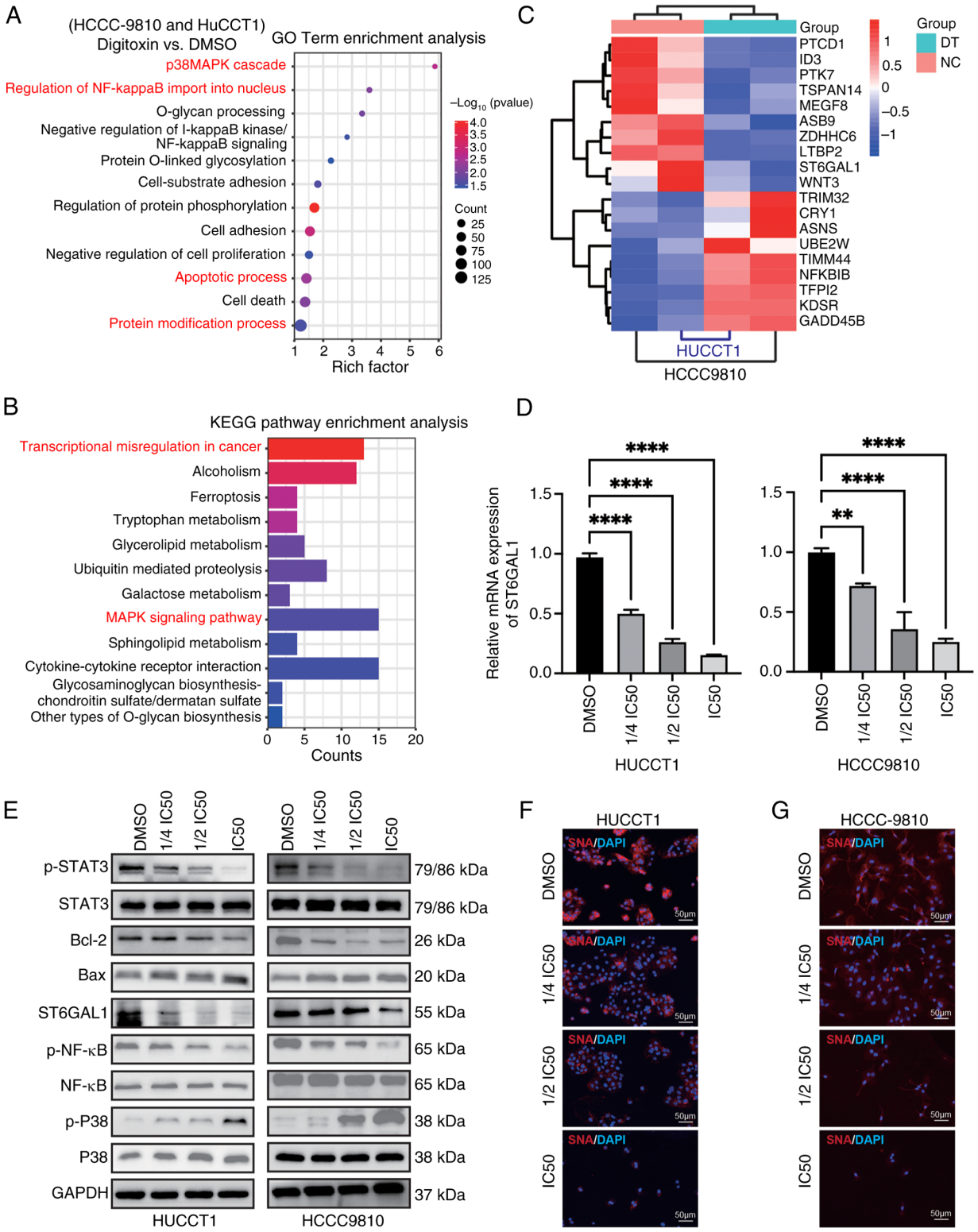

Figure 3. NF-κB/ST6GAL1 pathway plays a crucial role in the impact of DT on inhibiting the progression of ICC cells. (A) Enrichment analysis of GO terms. (B) Enrichment analysis of KEGG pathways. (C) Gene expression profiling alterations after DT treatment. (D) Reverse transcription-quantitative PCR was used to measure the expression levels of ST6GAL1 in ICC cells treated with DT. (E) Western blotting was employed to assess the expression levels of apoptosis-related proteins, NF-κB and ST6GAL1 following DT treatment. (F and G) In situ lectin fluorescence was used to detect the levels of α2,6-sialylation. Data are presented as the mean ± SD, representing the results of three independent experiments. **P<0.01 and ****P<0.0001. ST6GAL1, ST6 β-galactoside α-2,6-sialyltransferase 1; DT, digitoxin; ICC, intrahepatic cholangiocarcinoma; GO, Gene Ontology; KEGG, Kyoto Encyclopedia of Genes and Genomes.

and HuCCT1 cells were confirmed by RT-qPCR and western blotting (Fig. S4A and B). The colony formation and EdU assays provided compelling evidence that overexpression of ST6GAL1 significantly promotes the proliferation of ICC cells. These assays highlighted that ST6GAL1 could not only enhance cell proliferation, but also counteract the suppression

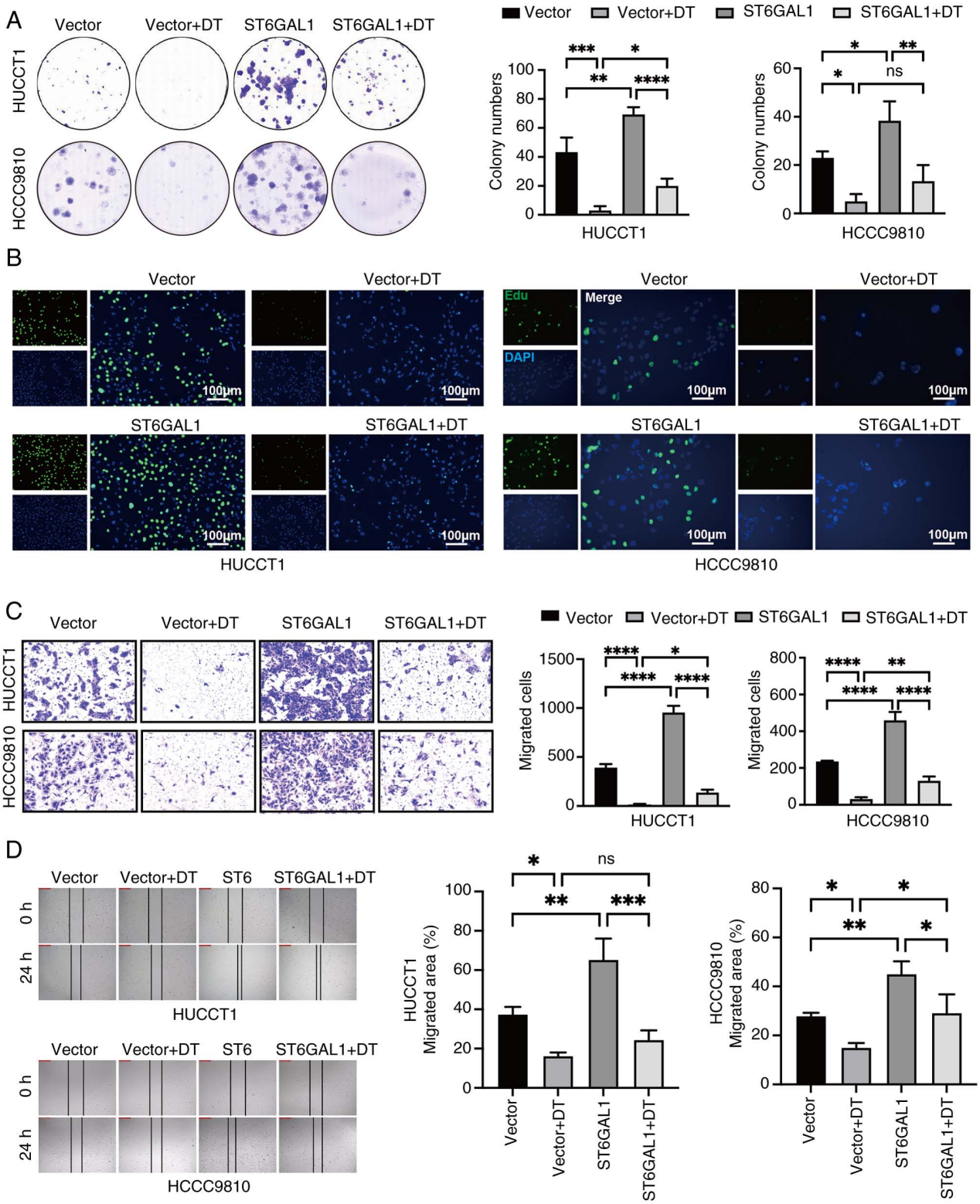

Figure 4. Elevated expression of ST6GAL1 counteracts the suppressive impact of DT on ICC cell proliferation and migration. (A) Overexpression of ST6GAL1 reversed the diminished colony-forming ability of ICC cells treated with DT. (B) Restoration of proliferation as evidenced by 5-ethynyl-2'-deoxyuridine incorporation. (C and D) Recovery of migration capabilities assessed by Transwell and wound healing assays. *P<0.05, **P<0.01, ***P<0.001 and ****P<0.0001. Error bars represent the mean ± SD obtained from three separate experiments. ST6GAL1, ST6 β-galactoside α-2,6-sialyltransferase 1; DT, digitoxin; ICC, intrahepatic cholangiocarcinoma; ns, no significance.

caused by DT (Fig. 4A and B). Further investigation into the impact of ST6GAL1 on cell migration was conducted using wound healing and Transwell migration assays. The outcomes from these assays confirmed that ST6GAL1 overexpression not only augmented the migratory capabilities of ICC cells, but also effectively neutralized the migration-inhibiting influence of DT (Fig. 4C and D). Collectively, these findings revealed that ST6GAL1 acted as a potent promoter of both proliferation

and migration of ICC cells, effectively reversing the inhibitory effects imposed by DT treatment.

DT inhibits ICC progression through the NF-κB/ST6GAL1 signaling pathway. To ascertain the critical role of ST6GAL1 in the signaling pathway through which DT inhibited ICC cells, ST6GAL1-overexpressing HCCC9810 and HuCCT1 cells were treated with DT at IC_{50} value. Western blotting results revealed that DT inhibited the expression of the anti-apoptotic protein Bcl-2, while overexpression of ST6GAL1 enhanced Bcl-2 expression and partially reversed the inhibitory effect of DT. Moreover, DT was shown to suppress ST6GAL1 expression in both control vector cells and ST6GAL-overexpressing cells (Fig. 5A and B). The aforementioned results indicated that DT could inhibit the phosphorylation of NF-κB, STAT3 and activate p-P38. Consequently, nuclear proteins were next extracted to examine the changes in nuclear p-NF-κB, p-STAT3 and p-P38 in ICC cells treated with DT at the IC_{50} concentration. Western blotting results suggested that DT could activate p-P38, and inhibit p-NF-κB and p-STAT3 in whole cells (Fig. 5A and B; statistical charts, Fig. S5A and B), and further nuclear protein detection revealed an increased expression of nuclear p-P38, and a decrease in p-NF-κB and p-STAT3 (Fig. 5C and D; statistical charts, Fig. S5C and D). In addition, SNA lectin flow cytometry was employed to evaluate the α2,6 sialylation levels in cells, with the aim of exploring the enzymatic activity of ST6GAL1. The experimental findings revealed that DT could reduce the α2,6 sialylation on the cell membrane, and the overexpression of ST6GAL1 was able to counteract the reduction effect induced by DT (Fig. 5E and F). These findings further elucidated that DT can modulate the expression of ST6GAL1 by impeding NF-κB activation, diminishing the nuclear presence of p-NF-κB and ultimately suppressing ICC cell progression through the downregulation of the effector protein Bcl-2.

Discussion

TCM plays an important role in cancer prevention and interception (17-19). TCM has long been used to maintain health and treat ailments. Growing evidence supports the use of TCM, alone or combined with other treatments, in reducing adverse effects associated with chemotherapy, improving the quality of life of patients, lowering the risk of recurrence and prolonging OS (20). In recent years, researchers have been increasingly interested in exploring potential anticancer compounds from TCM. Nobiletin, a major component of *Pericarpium Citri Reticulatae*, could inhibit cholangiocarcinoma (CCA) proliferation by direct binding to GSK3β (21). β-elemene, a potent component found in turmeric from the Chinese herbal medicine *Rhizoma Zedoariae*, has the potential to halt the advancement of CCA through the reactivation of PCDH9 expression (22). The screening results of the present study showed that DT, bufalin, neriifolin and telocinobufagin strongly suppressed ICC cell viability. DT, bufalin, neriifolin and telocinobufagin share common characteristics as cardiotonic steroids. They inhibit the plasma membrane Na^+/K^+-ATPase pumps leading to increased intracellular levels of Na^+ and Ca^+, decreased K^+ levels and enhanced cardiac contractile force (23). DT was isolated from the *Digitalis* species and features a steroid ring with a five-carbon unsaturated butyrolactone moiety (24,25). Bufadienolides such as bufalin, cinobufagin, telocinobufagin and others, found in *Venenum Bufonis* from toad species, possess a six-carbon unsaturated pyrone ring attached to the steroid ring (26,27). Among them, only DT has been approved by the FDA for specific cardiac conditions, particularly heart failure and certain heart arrhythmias. Consequently, the focus of the present study was on the possible therapeutic effects of DT on ICC.

The current study presented evidence from cellular functional assays indicating that DT effectively inhibited the proliferation and migration of ICC cells in a dose-dependent manner. Through GO and KEGG enrichment analyses, confirmed by RT-qPCR and western blotting validation, it was established that DT notably dampened the activation of the NF-κB signaling pathway, including its nuclear transcription activities, impeded the activation of p-STAT3 and activated the phosphorylation of P38. This was consistent with prior studies highlighting the ability of DT to inhibit p-STAT3 activation (28) and NF-κB (29). Additionally, while DT has been revealed to inhibit IL-1β-induced activation of p44/42-MAPK and NF-κB but not that of p38-MAPK in endothelial cells (30), the findings of the current study revealed that DT could activate p38-MAPK in ICC cells. During cellular stress, active p38 had been identified to phosphorylate and induce the degradation of BCL2 (31). Taken together, these findings revealed the role of DT as a comprehensive inhibitor of cancer progression by modulating critical signaling pathways pivotal to cancer cell growth and dissemination.

Sialylation is crucial in deciding cell destiny throughout development, reprogramming and cancer progression (32). The enzyme ST6GAL1, which catalyzes the attachment of α2,6-linked sialic acid to specific N-glycosylated proteins, either present on the cell membrane or secreted into the bloodstream, has been found to be upregulated in various cancers, where it promotes growth and invasiveness (33). Elevated levels of ST6GAL1 have also been linked to increased resistance to chemoradiotherapy in cancer models by inhibiting cell death (34). Furthermore, ST6GAL1 sourced from external environments can mimic the effects of endogenous proteins, fostering aggressive tumor proliferation and invasion (35). The present study demonstrated that ST6GAL1 overexpression could enhance ICC cell proliferation and migration, effectively countering the inhibition of proliferation and migration of DT. The engagement of NF-κB with the ST6GAL1 gene promoter initiates its transcription (16), a process inhibited by DT through the inhibition of NF-κB phosphorylation and nuclear translocation, leading to reduced ST6GAL1 mRNA and protein levels. Furthermore, it was demonstrated that overexpressing P65/NF-κB in 293T cells enhanced the expression of ST6GAL1. These findings indicated that DT impeded the progression of ICC by curtailing ST6GAL1 expression via the NF-κB pathway inhibition.

Despite DT being recognized as an essential drug by the World Health Organization, its potent activity and narrow therapeutic window pose significant challenges for clinical use (36). Adults should typically have therapeutic plasma DT value range of 10-30 ng/m (13.1-39.2 nM) (37). However, within the therapeutic concentration range of 25-40 nM, DT

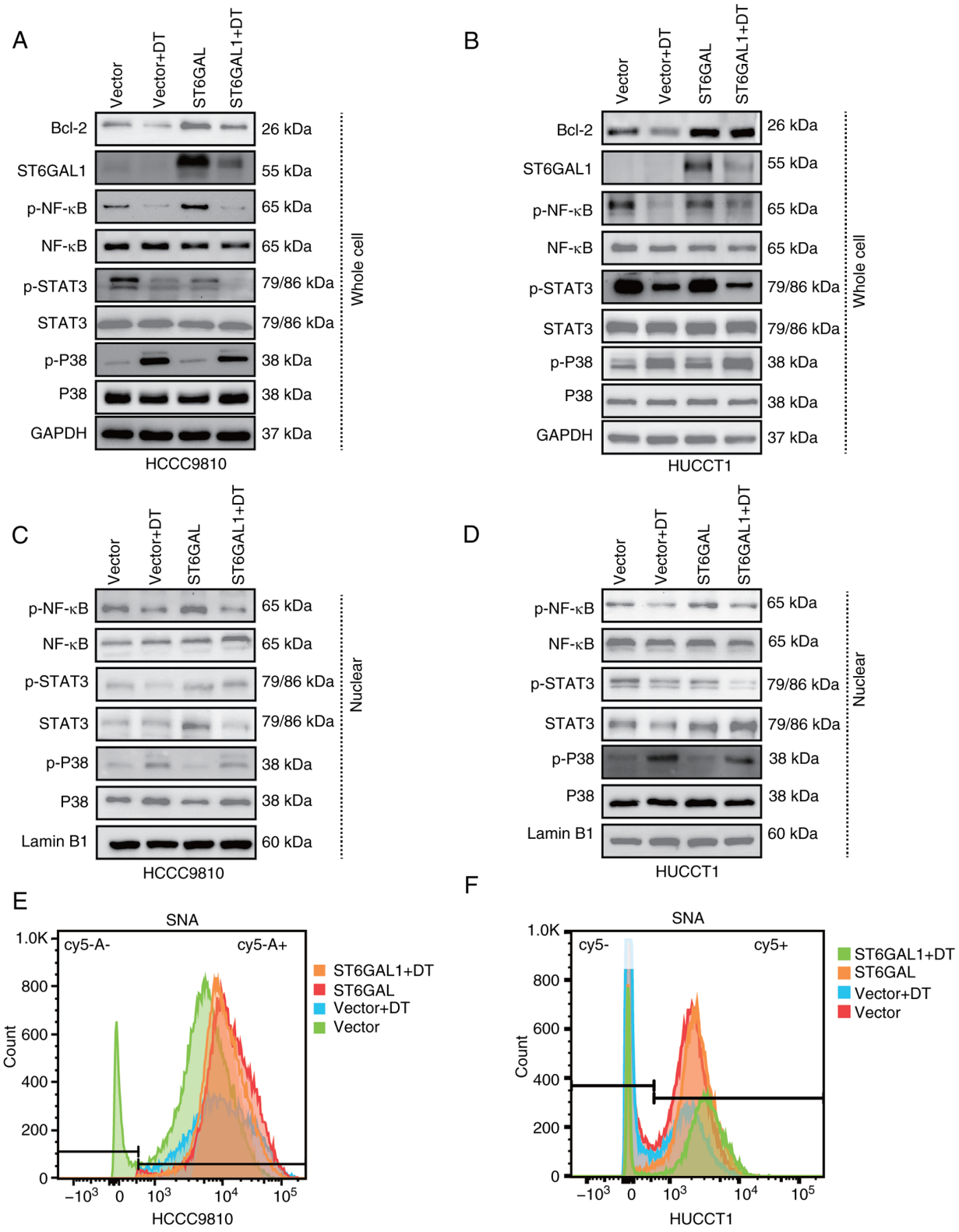

Figure 5. ST6GAL1 overexpression counteracts the signaling pathway involved in the DT-mediated effects in intrahepatic cholangiocarcinoma cells. (A and B) Western blots showing the protein profiles of ST6GAL1, Bcl-2, total STAT3, p-STAT3, total P38, p-P38, total NF-κB and p-NF-κB in HCCC9810 cells treated with DT. (C and D) Western blots showing the protein profiles of ST6GAL1, Bcl-2, total Akt, p-Akt, total P38, p-P38, total NF-κB and p-NF-κB in HuCCT1 cells treated with DT. (E and F) Flow cytometry was used to assess the levels of α2,6-sialylation in the different treatment groups. ST6GAL1, ST6 β-galactoside α-2,6-sialyltransferase 1; DT, digitoxin; p, phosphorylated.

demonstrates no marked adverse effects on normal cells, highlighting its potential for safe application (38,39). It is crucial to monitor for possible cardiac complications associated with DT, especially at serum concentrations indicative of toxicity. Evidence showed that a serum concentration range of 108-205 ng/ml (140-270 nM) might lead to DT poisoning (10).

However, the current study found that lower concentrations, specifically at half the IC_{50} value, were within a therapeutically effective range that demonstrated a significant inhibitory impact on ICC cells. Furthermore, previous studies have reported that DT can produce anticancer effects at concentration range of 20-33 nM without manifesting notable toxicity in patients with cardiac issues (40,41). Notably, there is a lack of research on the effects of DT on ICC. The findings of the current study indicated that a low concentration of DT, specifically at 1/4 IC_{50} value (23 nM for HCCC9810 and 26 nM for HuCCT1) at 48 h, fell within an effective range for exerting significant inhibitory effects on ICC cells. This observation was consistent with the previous studies of the anticancer efficacy of DT at concentrations that are not toxic. Furthermore, with a half-life range of 5-8 days in the human serum, DT provides a foundation for sustained tumor suppression (42).

In conclusion, DT, an effective anti-ICC compound, was identified from a TCM library. It was demonstrated that DT inhibited the progression of ICC by targeting ST6GAL1, a promoter of ICC growth. The findings of the current study revealed that DT downregulated ST6GAL1 at both the mRNA and protein levels in ICC cells and impeded NF-κB activation, which was crucial for the transcriptional activation of ST6GAL1. Therefore, the mechanism of DT in inhibiting ICC cell proliferation and metastasis was mediated through its interaction with the NF-κB/ST6GAL1 signaling pathway. These results not only emphasized the potential role of DT as a therapeutic agent for ICC, but also highlighted the critical function of ST6GAL1 in cancer progression. Nonetheless, a significant limitation of the present study was the lack of *in vivo* experiments to confirm the effectiveness of DT in treating ICC. Further investigation is necessary to comprehensively evaluate the *in vivo* effect.

Acknowledgements

Not applicable.

Funding

The present study was supported by the National Science Foundation of China (grant no. 82372321), the Shanghai Shenkang Hospital Development Center Project (grant no. SHDC2023CRT015) and the Shanghai 'Rising Stars of Medical Talent' Youth Development Program (grant no. 2024-70).

Availability of data and materials

The data generated in the present study are included in the figures and/or tables of this article. The RNA-seq data generated in the present study may be found in the SRA database under accession number PRJNA1112815 or at the following URL: https://www.ncbi.nlm.nih.gov/sra/PRJNA1112815.

Authors' contributions

CG conceived and directed the project, and designed the experiments. YZ, RW, CH, XXu, XXi, LW, JW and TL carried out the experiments. YZ and RW conducted the data analysis and interpreted the results. YZ and CG wrote and edited the manuscript, and confirm the authenticity of all the raw data. All authors read and approved the final manuscript.

Ethics approval and consent to participate

The requirement for the ethics approval of purchased primary human cells was waived by the Ethics Committee of Yueyang Integrated Traditional Chinese and Western Medicine Affiliated with Shanghai University of Traditional Chinese Medicine in accordance with Article 32 of the Chinese Measures for the Ethical Review of Life Science and Medical Research Using Humans.

Patient consent for publication

Not applicable.

Competing interests

The authors declare that they have no competing interests.

References

1. Siegel RL, Miller KD, Fuchs HE and Jemal A: Cancer statistics, 2022. CA Cancer J Clin 72: 7-33, 2022.
2. Beal EW, Tumin D, Moris D, Zhang XF, Chakedis J, Dilhoff M, Schmidt CM and Pawlik TM: Cohort contributions to trends in the incidence and mortality of intrahepatic cholangiocarcinoma. Hepatobiliary Surg Nutr 7: 270-276, 2018.
3. Lee YT, Wang JJ, Luu M, Noureddin M, Nissen NN, Patel TC, Roberts LR, Singal AG, Gores GJ and Yang JD: Comparison of clinical features and outcomes between intrahepatic cholangiocarcinoma and hepatocellular carcinoma in the United States. Hepatology 74: 2622-2632, 2021.
4. Abdel-Rahman O, Elsayed Z and Elhalawani H: Gemcitabine-based chemotherapy for advanced biliary tract carcinomas. Cochrane Database Syst Rev 4: CD011746, 2018.
5. Pellino A, Loupakis F, Cadamuro M, Dadduzio V, Fassan M, Guido M, Cillo U, Indraccolo S and Fabris L: Precision medicine in cholangiocarcinoma. Transl Gastroenterol Hepatol 3: 40, 2018.
6. Cragg GM and Newman DJ: Natural products: A continuing source of novel drug leads. Biochim Biophys Acta 1830: 3670-3695, 2013.
7. Harvey AL, Edrada-Ebel R and Quinn RJ: The re-emergence of natural products for drug discovery in the genomics era. Nat Rev Drug Discov 14: 111-129, 2015.
8. Newman DJ and Cragg GM: Natural products as sources of new drugs from 1981 to 2014. J Nat Prod 79: 629-661, 2016.
9. Trenti A, Zulato E, Pasqualini L, Indraccolo S, Bolego C and Trevisi L: Therapeutic concentrations of digitoxin inhibit endothelial focal adhesion kinase and angiogenesis induced by different growth factors. Br J Pharmacol 174: 3094-3106, 2017.
10. Patel S: Plant-derived cardiac glycosides: Role in heart ailments and cancer management. Biomed Pharmacother 84: 1036-1041, 2016.
11. Zhang YZ, Chen X, Fan XX, He JX, Huang J, Xiao DK, Zhou YL, Zheng SY, Xu JH, Yao XJ, *et al*: Compound library screening identified cardiac glycoside digitoxin as an effective growth inhibitor of gefitinib-resistant non-small cell lung cancer via downregulation of alpha-tubulin and inhibition of microtubule formation. Molecules 21: 374, 2016.
12. Lee DH, Lee CS, Kim DW, Ae JE and Lee TH: Digitoxin sensitizes glioma cells to TRAIL-mediated apoptosis by upregulation of death receptor 5 and downregulation of survivin. Anticancer Drugs 25: 44-52, 2014.
13. Liu M, Feng LX, Sun P, Liu W, Mi T, Lei M, Wu W, Jiang B, Yang M, Hu L, *et al*: Knockdown of Apolipoprotein E Enhanced sensitivity of Hep3B cells to cardiac steroids via regulating Na+/K+-ATPase signalosome. Mol Cancer Ther 15: 2955-2965, 2016.

14. Pollard BS, Suckow MA, Wolter WR, Starr JM, Eidelman O, Dalgard CL, Kumar P, Battacharyya S, Srivastava M, Biswas R, *et al*: Digitoxin inhibits Epithelial-to-Mesenchymal-Transition in hereditary castration resistant prostate cancer. Front Oncol 9: 630, 2019.
15. Livak KJ and Schmittgen TD: Analysis of relative gene expression data using real-time quantitative PCR and the 2(-Delta Delta C(T)) method. Methods 25: 402-408, 2001.
16. Fan Q, Li M, Zhao W, Zhang K, Li M and Li W: Hyper alpha2,6-sialylation promotes CD4(+) T-cell activation and induces the occurrence of ulcerative colitis. Adv Sci (Weinh) 10: e2302607, 2023.
17. Ye L, Jia Y, Ji KE, Sanders AJ, Xue K, Ji J, Mason MD and Jiang WG: Traditional Chinese medicine in the prevention and treatment of cancer and cancer metastasis. Oncol Lett 10: 1240-1250, 2015.
18. Xiang Y, Guo Z, Zhu P, Chen J and Huang Y: Traditional Chinese medicine as a cancer treatment: Modern perspectives of ancient but advanced science. Cancer Med 8: 1958-1975, 2019.
19. Yan Z, Lai Z and Lin J: Anticancer properties of traditional Chinese medicine. Comb Chem High Throughput Screen 20: 423-429, 2017.
20. Wu HA, Chen CH, Hsieh MH, Wu YC, Chiu JP, Huang CJ and Hsu CH: The Benefit of Enhanced daycare of traditional Chinese medicine for cancer treatment related adverse events: A retrospective study of medical records. Integr Cancer Ther 20: 15347354211025634, 2021.
21. You L, Lin J, Yu Z, Qian Y, Bi Y, Wang F, Zhang L, Zheng C, Zhang J, Li W, *et al*: Nobiletin suppresses cholangiocarcinoma proliferation via inhibiting GSK3β. Int J Biol Sci 18: 5698-5712, 2022.
22. Wu Q, Shi X, Pan Y, Liao X, Xu J, Gu X, Yu W, Chen Y and Yu G: The chemopreventive role of β-Elemene in cholangiocarcinoma by restoring PCDH9 expression. Front Oncol 12: 874457, 2022.
23. Wang JKT, Portbury S, Thomas MB, Barney S, Ricca DJ, Morris DL, Warner DS and Lo DC: Cardiac glycosides provide neuroprotection against ischemic stroke: Discovery by a brain slice-based compound screening platform. Proc Natl Acad Sci USA 103: 10461-10466, 2006.
24. Prassas I and Diamandis EP: Novel therapeutic applications of cardiac glycosides. Nat Rev Drug Discov 7: 926-935, 2008.
25. Botelho AFM, Pierezan F, Soto-Blanco B and Melo MM: A review of cardiac glycosides: Structure, toxicokinetics, clinical signs, diagnosis and antineoplastic potential. Toxicon 158: 63-68, 2019.
26. Wei WL, An YL, Zhang YZ, Li ZW, Zhou Y, Lei M, Zhang JQ, Qu H, Da J, Wu WY and Guo DA: Quantitative analysis of fourteen bufadienolides in *Venenum bufonis* crude drug and its Chinese patent medicines by ultra-high performance liquid chromatography coupled with tandem mass spectrometry. J Ethnopharmacol 251: 112490, 2020.
27. Kumavath R, Paul S, Pavithran H, Paul MK, Ghosh P, Barh D and Azevedo V: Emergence of cardiac glycosides as potential drugs: Current and future scope for cancer therapeutics. Biomolecules 11: 1275, 2021.
28. Mi C, Cao X, Ma K, Wei M, Xu W, Lin Y, Zhang J and Wang TY: Digitoxin promotes apoptosis and inhibits proliferation and migration by reducing HIF-1α and STAT3 in KRAS mutant human colon cancer cells. Chem Biol Interact 351: 109729, 2022.
29. Eldawud R, Wagner A, Dong C, Gupta N, Rojanasakul Y, O'Doherty G, Stueckle TA and Dinu CZ: Potential antitumor activity of digitoxin and user-designed analog administered to human lung cancer cells. Biochim Biophys Acta Gen Subj 1864: 129683, 2020.
30. Jagielska J, Salguero G, Schieffer B and Bavendiek U: Digitoxin elicits anti-inflammatory and vasoprotective properties in endothelial cells: Therapeutic implications for the treatment of atherosclerosis? Atherosclerosis 206: 390-396, 2009.
31. Whitaker RH and Cook JG: Stress relief techniques: p38 MAPK determines the balance of cell cycle and apoptosis pathways. Biomolecules 11: 1444, 2021.
32. Li F and Ding J: Sialylation is involved in cell fate decision during development, reprogramming and cancer progression. Protein Cell 10: 550-565, 2019.
33. Scott E, Archer Goode E, Garnham R, Hodgson K, Orozco-Moreno M, Turner H, Livermore K, Putri Nangkana K, Frame FM, Bermudez A, *et al*: ST6GAL1-mediated aberrant sialylation promotes prostate cancer progression. J Pathol 261: 71-84, 2023.
34. Smithson M, Irwin R, Williams G, Alexander KL, Smythies LE, Nearing M, McLeod MC, Al Diffalha S, Bellis SL and Hardiman KM: Sialyltransferase ST6GAL-1 mediates resistance to chemoradiation in rectal cancer. J Biol Chem 298: 101594, 2022.
35. Hait NC, Maiti A, Wu R, Andersen VL, Hsu CC, Wu Y, Chapla DG, Takabe K, Rusiniak ME, Bshara W, *et al*: Extracellular sialyltransferase st6gal1 in breast tumor cell growth and invasiveness. Cancer Gene Ther 29: 1662-1675, 2022.
36. Ambrosy AP and Gheorghiade M: Targeting digoxin dosing to serum concentration: Is the bullseye too small? Eur J Heart Fail 18: 1082-1084, 2016.
37. Belz GG, Breithaupt-Grogler K and Osowski U: Treatment of congestive heart failure-current status of use of digitoxin. Eur J Clin Invest 31 (Suppl 2): S10-S17, 2001.
38. Lopez-Lazaro M, Pastor N, Azrak SS, Ayuso MJ, Cortes F and Austin CA: Digitoxin, at concentrations commonly found in the plasma of cardiac patients, antagonizes etoposide and idarubicin activity in K562 leukemia cells. Leuk Res 30: 895-898, 2006.
39. Bavendiek U, Berliner D, Dávila LA, Schwab J, Maier L, Philipp SA, Rieth A, Westenfeld R, Piorkowski C, Weber K, *et al*: Rationale and design of the DIGIT-HF trial (DIGitoxin to Improve ouTcomes in patients with advanced chronic Heart Failure): A randomized, double-blind, placebo-controlled study. Eur J Heart Fail 21: 676-684, 2019.
40. Lopez-Lazaro M, Pastor N, Azrak SS, Ayuso MJ, Austin CA and Cortes F: Digitoxin inhibits the growth of cancer cell lines at concentrations commonly found in cardiac patients. J Nat Prod 68: 1642-1645, 2005.
41. Daniel D, Susal C, Kopp B, Opelz G and Terness P: Apoptosis-mediated selective killing of malignant cells by cardiac steroids: Maintenance of cytotoxicity and loss of cardiac activity of chemically modified derivatives. Int Immunopharmacol 3: 1791-1801, 2003.
42. Bohmer T and Roseth A: Prolonged digitoxin half-life in very elderly patients. Age Ageing 27: 222-224, 1998.